Investigation of anti-reflective silicon nitride (Si_3N_4) thin film: A CVD technique

M. GEETHA[1], R.S. DUBEY[2], S. SARAVANAN[3,*]
[1]*Department of Physics(S&H), R P Sarathy Institute of Technology, Salem (TN)- 636 305, India*
[2]*Department of CS&AI, SR University, Warangal, Telangana, India*
[3]*Department of Physics (S&H), Swarnandhra College of Engineering and Technology (A),Seetharampuram, Narsapur-534280, West Godavari (AP), India*

In this work, the fabrication of Si_3N_4 thin films using the chemical vapor deposition technique. The fabricated Si_3N_4thin film investigated their reflectance, structural, functional, and topographical properties usingvariouscharacterization techniques. UV-visible spectra are evidencing the successful and improvement of anti-reflection coating properties at nanoscale engineering by reporting the lowest reflection (15%). XRD pattern revealed the sharp diffraction peaks and confirmed the presence of crystalline and α-Si_3N_4phases. Furthermore, 3D- AFM topographyhadshownthesample surface area of the scanning surface of 1x1μm^2. These topography results are including thin film in the heights of 25, 4.2, and 24.2 nm with the corresponding surface area ratios of 2.8, 2.2, and 2.3%. Overall, the obtained properties are well-suited and useful in thin film solar cells as better anti-reflection coating to reduce the reflection of incoming light and could be boost the absorption of incoming photons by harvesting mechanism.

(Received August 21, 2024; accepted August 5, 2025)

*Keywords:*Thin film, CVD, Si_3N_4, XRD, AFM, ARC

1. Introduction

The silicon nitride (Si_3N_4) thin films are useful in a variety of important technological applications due to their unique antireflective coatings, high corrosion resistance, the passivation layer, isolation of semiconductor devices, and high chemical and thermal stability [1–2].It plays pivotal role in silicon-based photonics and photonic quantum computing. Chemical vapor deposition (CVD), plasma enhanced CVD (PECVD), atomic layer deposition (ALD), RF magnetron sputtering, and radio frequency PECVD (RF-PECVD), are useful for the fabrication of Si_3N_4coatings [3-6]. Among these techniques, CVD is one of the preferred techniques for its low-cost and highest precise control. The various researchers reported the significance of Si_3N_4 and SiO_2 using CVD techniques. Chee et al. (2018) demonstrated the effect of various anti-reflective coatings (ZnO, SiO_2/Si_3N_4, and surface texturing) structures in the silicon solar cells using finite-element modeling and magnetron sputtering deposition techniques. The single-ZnO and double (SiO_2/Si_3N_4) layers of optimized thickness calculated reduced reflectivity. Under normal light incidence, ZnO, SiO_2/Si_3N_4, and surface texture increased the cell efficiency by 20%, 24%, and 30%[7].Ahmed et al. (2013)investigated the Raman and Fourier infrared techniques (FTIR) studies of ammonia free, hydrogenated amorphous silicon nitride (a-SiN_x:H) thin films, which were fabricated by plasma enhanced chemical vapor deposition techniques. FTIR vibrational modes between 780 and 800 cm^{-1} and Raman spectroscopy analysis confirmed the presence of Si-Si and Si-N bonds around 400 and 480 cm^{-1}. Further, deposited thin film refractive indices (2.0–3.75) were calculated using optical transmittance spectra and Swanepoel's method [8].Lee and Ku(2010)fabricated the Si_3N_4 and SiO_2 thin films by ion-assisted deposition technique for anti-reflection coating (ARC) applications. The amorphous structure, density, stoichiometric thin films, and low hydrogen content with desired optical properties were shown by XRD, transmission electron microscopy (TEM), FTIR, and ellipsometry studies. Overall, excellent optical interference coating capability was achieved in the infrared region [9].Swatowska et al. (2011) presented the role of different anti-reflective coatings (a-Si:C:H, a-Si:N:H, andTiO_2) in silicon solar cells using PECVD techniques. Among these anti-reflection coatings, the favored a-Si:N:H thin film layer showed an improved reflectivity coefficient (Reff = 8.3%) and conversion cell efficiency of 14.25% [10].Hashmi et al. (2018)numerically studied the impact of different anti-reflection coatings (ARC) layers using PC1D software tools. The single layer of Si_3N_4 ARC layer was designed with a 74.257 nm thickness and 600 nm wavelengths, which was integrated into silicon solar cells and achieved 20.35% efficiency. Further, a zinc oxide ARC layer with 74.87 nm thickness generated a 20.34% efficient Si solar cell. Finally, surface passivation of SiO_2/Si_3N_4, ARC layers highly achieved 20.67% cell efficiency [11]. Sahoo et al.(2009) studied the reflectance property of Si_3N_4 sub-wavelength structures (SWS) for thin film silicon solar cells. Numerical calculation of Si_3N_4 antireflection coatings investigated by rigorous coupled wave analysis (RCWA) method. The obtained results were compared with the fabricated samples (single- and double-layer anti-reflection (SLAR, DLAR) coatings) using a self-assembled and mask less reactive ion etching process. The experimental validated simulation showed significant cell efficiency enhancement of 0.2%

with Si_3N_4SWS height 140 nm and non-etched layer 60 nm [12]. Dubey et al. (2017) reported the investigation of multilayer thin film of SiO_2/Si_3N_4 and grating for solar cell applications. They experimentally (CVD method) demonstrated ~0.7% of absorption and simulated (RCWA method) thin film solar cells.It is garnering great interest on thin film solar cell [14]. The aim of this work is to study the structural, optical, topography, and functional groups of the prepared Si_3N_4 thin film. It was deposited on a silicon (Si) wafer (P-type) by using the chemical vapor deposition technique using nitrogen (N_2 gas), ammonia (NH_3 gas), and hexamethyldisiloxane (HMDSO) solutions. In this paper, we fabricated Si_3N_4 thin film using chemical vapor deposition techniques under atmospheric pressure condition. Our aim is to reduce the reflection properties for the betterment of anti-reflection coating in thin film solar cell applications. With this fabrication of Si_3N_4 thin film maintained the distance of 2 cm between each sample to know the deposition rate. This work is unique and not reported by any research community. Significantly, we achieved less than 15% reflection as per the literature survey. These materials highly reported 20.67% of cell efficiency and this can enhance with optimized Si_3N_4 thin film. Majorly, the reflection should be decreased on Si_3N_4 samples and absorption should be enhanced within the absorber or active region. We employed the starting materials, and experimental parameters are explored in Section 2. The obtained results of optical (UV-Visible Spectrometer), topographical (AFM), and structural (XRD) and functional (RAMAN, FTIR) properties of prepared thin films are discussed in Section 3. Finally, concludes the work in Section 4.

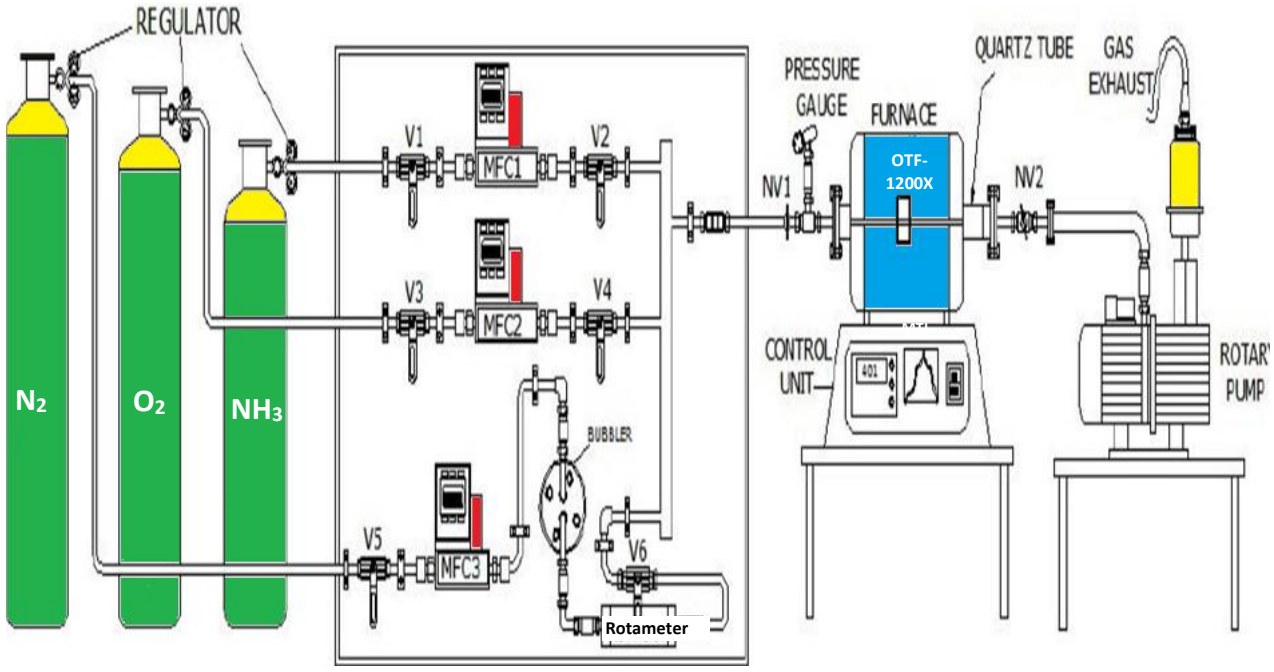

Fig. 1. The schematic diagram of the CVD system (colour online)

2. Experimental approach

2.1. Materials

The objective of this work is to study the α-Si_3N_4 properties. The CVD system is manufactured by MTI Corporation (Model-OTF 1200X). The following starting materials were used: hexamethyldisiloxane (HMDSO), silicon wafer (P-type substrate), ammonia (NH_3), oxygen (O_2), and nitrogen (N_2) gases are the primary sources of the Si_3N_4 thin film. Also, the silicon substrate can be ultrasonically cleaned by ethanol (C_2H_5OH), distilled water (H_2O), and acetone (C_3H_6O) to remove the residue such as grease, oil, etc.

2.2. Methods

The silicon nitride thin films were deposited on silicon substrates by using chemical vapor deposition (CVD), a schematic of which is shown in Fig. 1. The CVD system mainly consists of the following components: a quartz reactor, furnace, bubblers holding the reacting chemical solution, gas feed lines (O_2, N_2, NH_3), gas exit molecule, mass flow controller (MFC), rotary pump, and pressure gauge.

Table 1. Process parameters used for the deposition of Si_3N_4 thin films using CVD method

S.N.	Process Parameters	Value
1	Deposition Temperature (°C)	800
2	Distance Between the silicon Substrates (cm)	2
3	Ammonia (NH_3),flow rate (sccm)	90
4	Nitrogen (N_2), flow rate (sccm)	100
5	Deposition Time (t)	30 min
6	Temperature steps(°C)	200/10 min.
7	Hexamethyldisiloxane (HMDSO, $C_6H_{18}OSi_2$), ml	150

This chemical vapor deposition is a basic process for the deposition of SiO_2 and Si_3N_4. Before the deposition, the p-type silicon substrates were rinsed with distilled water (H_2O), ethanol, and methanol using the ultrasonication process. The substrates were loaded, and the deposition chamber was baked up to 800°C for 40 minutes. The thin films were prepared by using silicon sources as hexamethyldisiloxane (HMDSO). By using mass flow controllers (MFCs), we controlled the flow rate of ammonia (NH_3, 90 sccm) and nitrogen (N_2, 100 sccm), which is the source of the nitrogen. During the experimental work, the quartz tube's (length = 40 cm and width = 5 cm) pressure was observed by connecting a pressure gauge (μPa). The silicon wafer substrates were held at a constant temperature of 800 °C, and other parameters are tabulated (Table 1). The chamber was used for the deposition process into which the reactant gases are introduced to decompose and react with the silicon wafers (substrates). The silicon substrates (named as G, H, K, and L samples) were kept at a 2 cm distance. These distances maintained to know the quality of the deposition which is no one reported on this CVD method. It may play crucial role to fabricate the optimized or better anti-reflection coating in various applications like solar cell. The reactant gases were controlled by MFCs. Finally, the formation of non-volatile thin films grown on the silicon substrates is as follows:

$$2NH_3 + N_2 + C_6H_{18}OSi_2 + Si \rightarrow Si_3N_4 + C_6H_{12}O + 6H_2 \uparrow$$

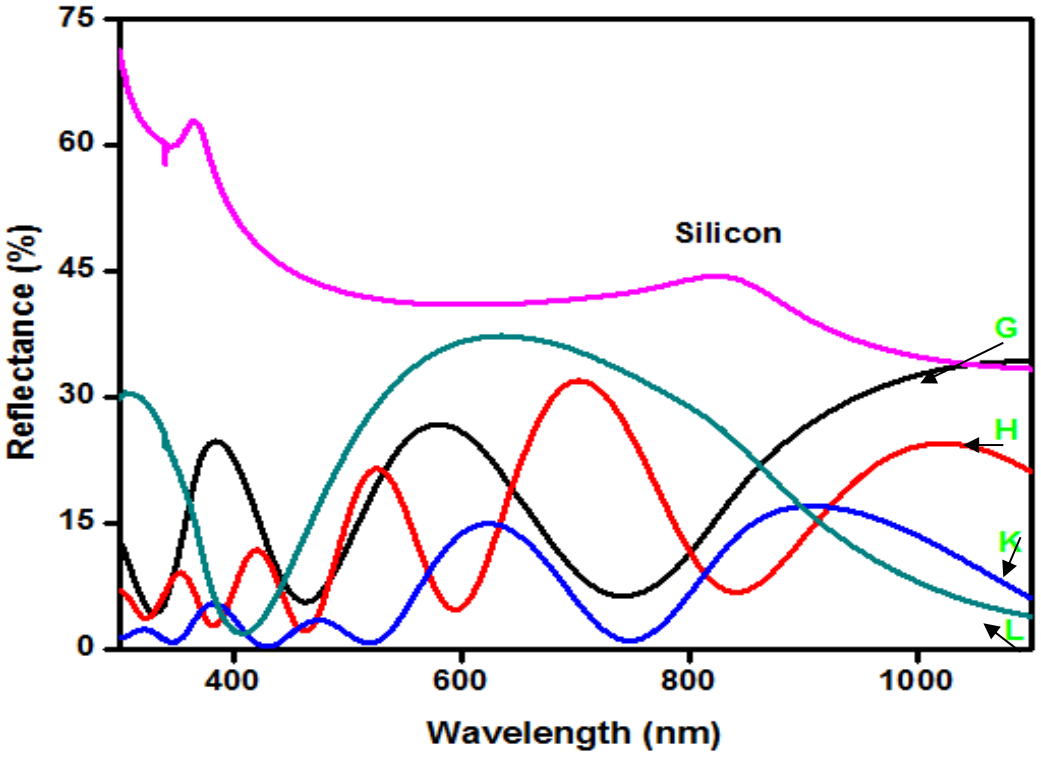

Fig. 2. Reflectance measurement on a Si_3N_4 coated silicon wafer (colour online)

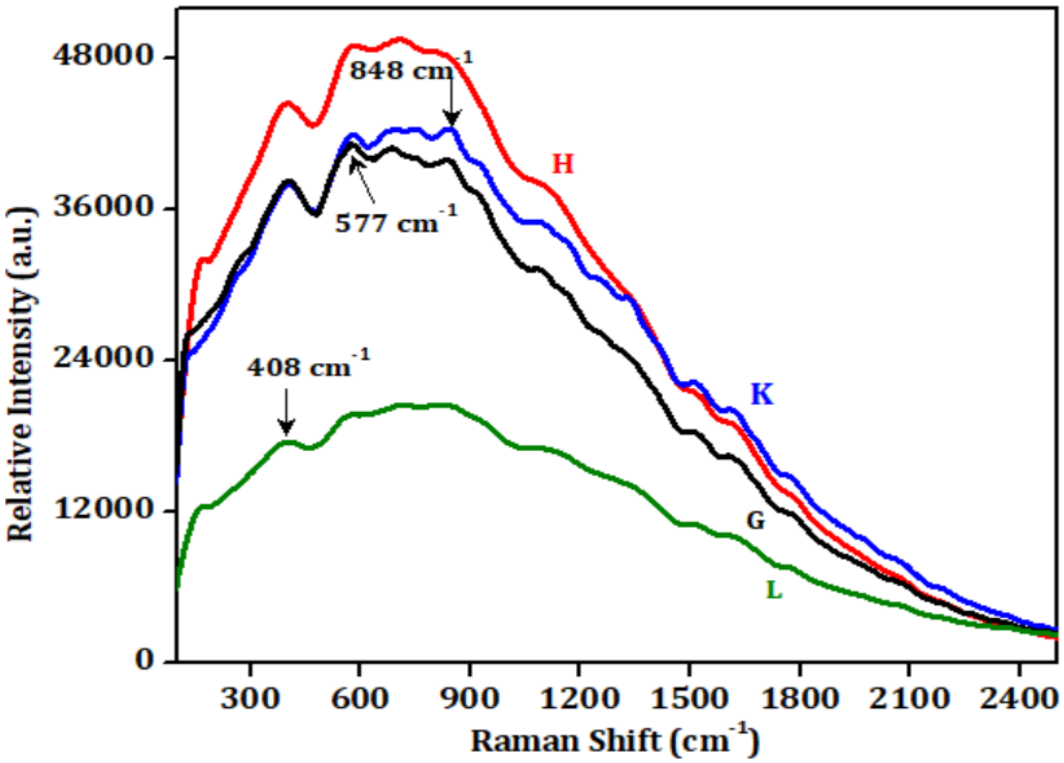

Fig.3. The Raman spectrum of Si_3N_4 thin films (colour online)

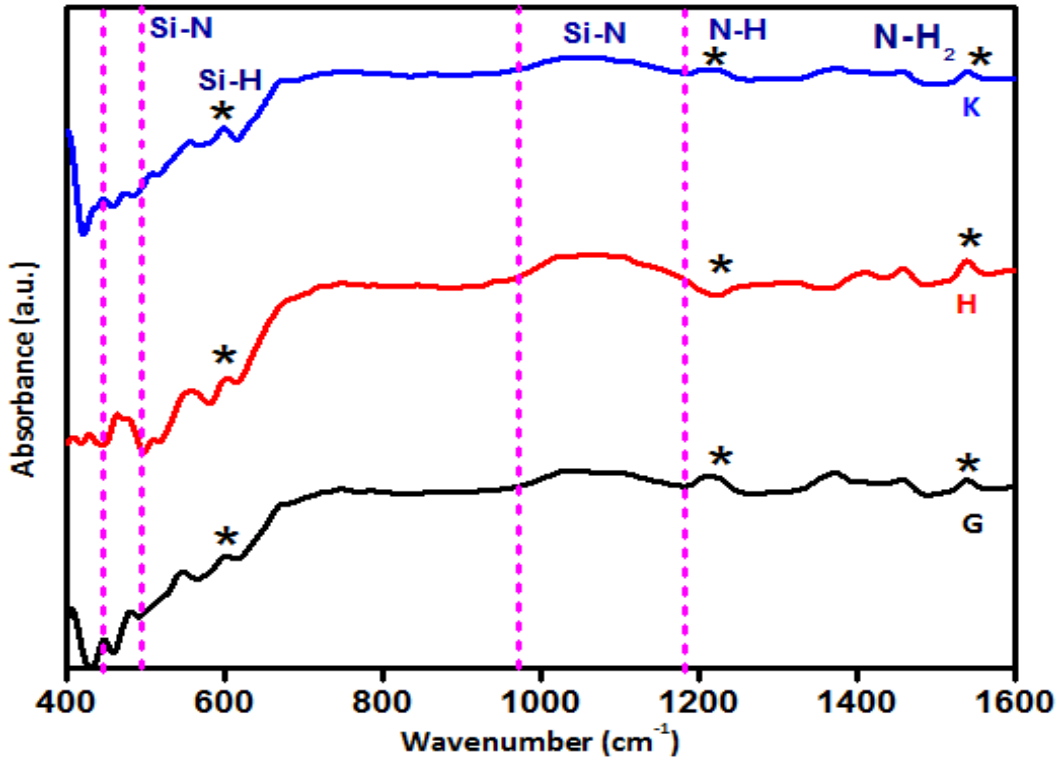

Fig.4.The Fourier transforms infrared spectra of Si_3N_4 thin films (colour online)

2.3. Characterization

In order to get the optical and structural performance, the prepared Si_3N_4 coated thin films were measured for their optical and morphological properties. Also, the reflectivity, elemental, surface roughness, and functional groups were measured by UV-visible spectrophotometers (UV-1800, Shimadzu, Japan), micro-Raman spectroscopy, X-ray diffractometers (XRD), Fourier transform infrared (FTIR,

Perkin Elmer, Spectrum 2) spectroscopy and atomic force microscopy (XE7-Park Systems, AFM).

3. Results anddiscussion

We fabricated four different silicon nitride thin films on silicon wafers using CVD techniques and studied their optical, functional, structural, and topography properties by using different characterization techniques as follows,

3.1. UV-visible spectroscopy

The measured reflectance of the Si_3N_4 coated silicon wafer is shown in Fig. 2. The variations of reflectance (vs. wavelength) of bare Si and Si_3N_4-coated silicon wafers are included. Before the CVD processing, each sample was maintained 2 cm from one another from the quartz tube. The refractive indices of Si_3N_4 (n = 1.87) calculated with respect to thumb rule ($n_{arc} = \sqrt{n_m n_{si}}$) as reported by Jhansirani et al. (2016)[13]. Here, 'n_{arc}' is the refractive index, 'n_m' is the atmospheric condition, and 'n_{si}' is the assumption of the silicon refractive index.

In this study, all the coated samples achieved minimum reflection as compared to bare silicon wafer. With the effect of distance (2 cm between each sample), the reflection intensity decreased considerably due to the reduced nanoscale thickness of thin films. Similarly, the reflectance decreases with respect to thin film thickness and the 'N' number of oscillations in the ultraviolet and visible spectral regions [15]. These oscillations are based on various parameters like angle of light incidence, absorption of thin film, and non-uniformity of the film. Similarly, Amotchkina et al.(2012)proved it with the simulation models and measurement techniques [16]. With the addition of low reflection, good surface passivation is achieved, as reported by various literatures [17].

3.2. Raman spectroscopy: functional

Raman (or Micro Raman) spectroscopy is a tool for characterization of microelectronic materials and device structures. Fig. 3shows the Raman spectrum of prepared Si_3N_4 thin film. These are identical, indicating that the samples are homogenous. These Raman spectra present the less intensity peaks with broad. Here, during the deposition of Si_3N_4, the ceramic powders over Si substrate appeared a few broader peaks, such as 408 (E_{2g}), 577 (Eg), and 848 cm^{-1} (A_{1g}), confirming α-Si_3N_4 [18].

3.3. Fourier transform infrared (FTIR): functional

The FTIR technique is a versatile and powerful analytical tool to obtain an infrared transmittance spectrum of the prepared Si_3N_4 thin films due to its sensitivity, speed, and ability to generate detailed information about the samples.The infrared radiation is absorbing the molecules (thin film) and noticing that the functional group of the samples is affected by vibrational modes. Fig. 4shows the chemical species bonding of the as-deposited Si_3N_4 thin films on the silicon wafer surfaces. The deposited thin films exhibit the characteristic features of Si_3N_4, such as Si-H and N-H stretching modes verified at 601 and 1200cm^{-1}. The strong absorption of Si-N stretching modes was noticed at 480 and 1056 cm^{-1}. The weak absorption peak of the N-H_2 wagging mode presented at 1541cm^{-1}. In this FTIR absorbance spectrum for the prepared samples, centered about the Si_3N_4. The prominent characteristic in the spectra is the shoulder from 970 to 1194 cm^{-1}. Because of the shoulder, the intensity of the peak increased at 480 cm^{-1} [19].

3.4. X-ray diffraction (XRD): structural

The structural properties of the prepared silicon nitride (Si_3N_4) thin film samples are investigated by X-ray diffraction techniques. The X-ray diffractograms of the samples (G and H) of Si_3N_4 thin films are shown in Fig. 5(a) and (b). At higher temperatures, the deposition rate is increasing, and temperature is responsible for the nucleate having more silicon nitride along their orientations. The obtained data were collected under the wavelength of 1.54060A°. The exclusive presence of Si_3N_4 is presented at (201), (301), and (321) [20-21]. The development of sharp diffraction peaks confirms their existence and is related to α-Si_3N_4 phase. The intensity of diffraction peaks is depicting the re-crystallization of silicon nitride at the nanoscale level. The secondary crystalline phases were forming during the cooling, indicating the amorphous nature within the grain boundary regions [22]. These results are confirming that the available species have suitable energy to interact with the silicon wafer by nucleation process along with their orientations. The growth and development of residual stresses are directly influenced by the nitrogen gases, which play a pivotal role in the development of nitride films.

3.5. Atomic force microscopy (AFM): topography

Fig. 6 shows the surface topography of Si_3N_4/Si thin films of three samples K, G, and H by using atomic force microscopy (3D).

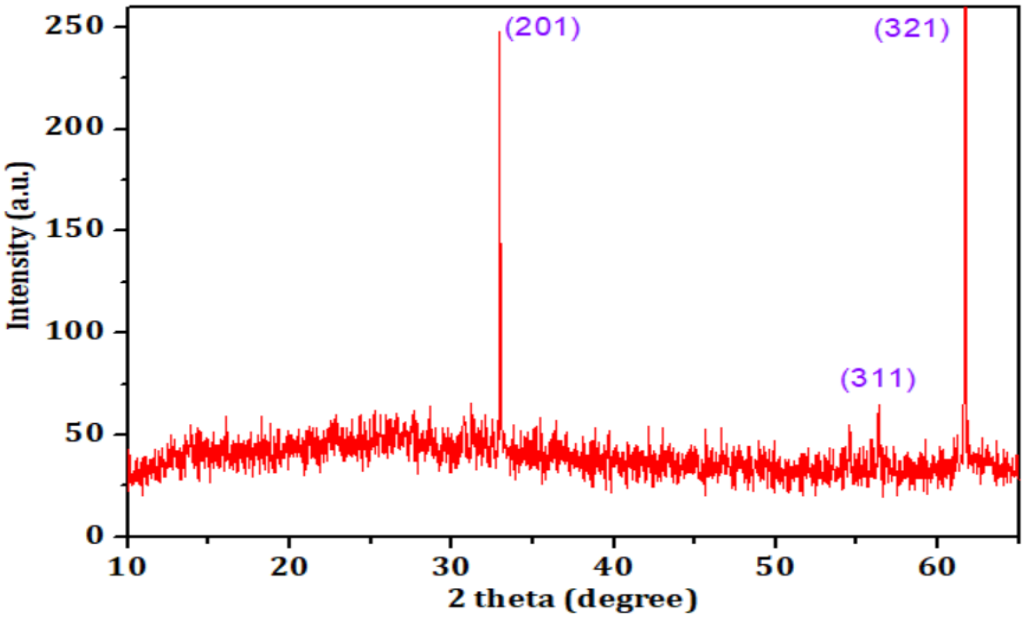

(a)

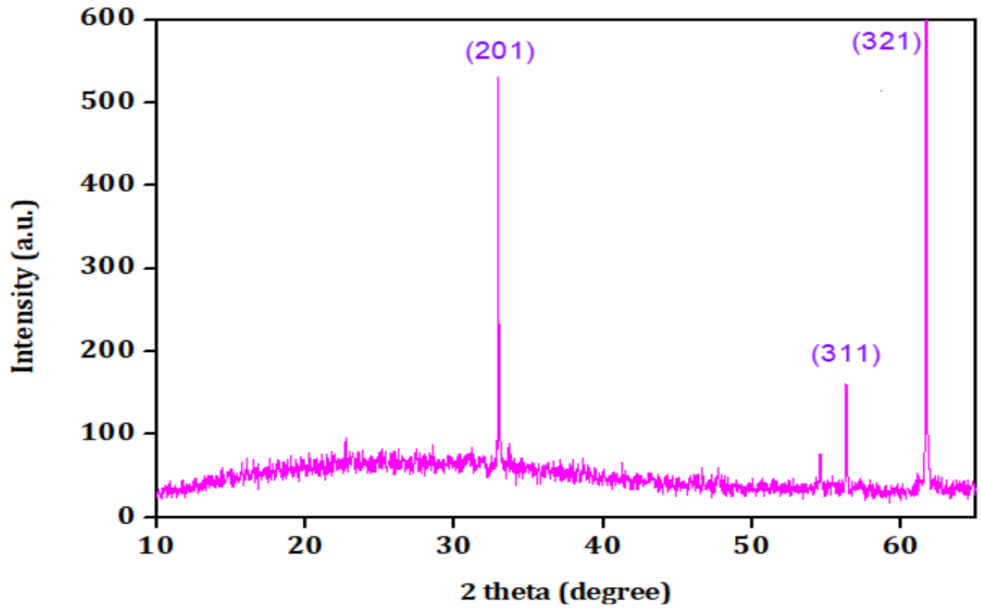

(b)

Fig.5. XRD pattern of Si_3N_4 thin film (a) G sample and (b) H sample (colour online)

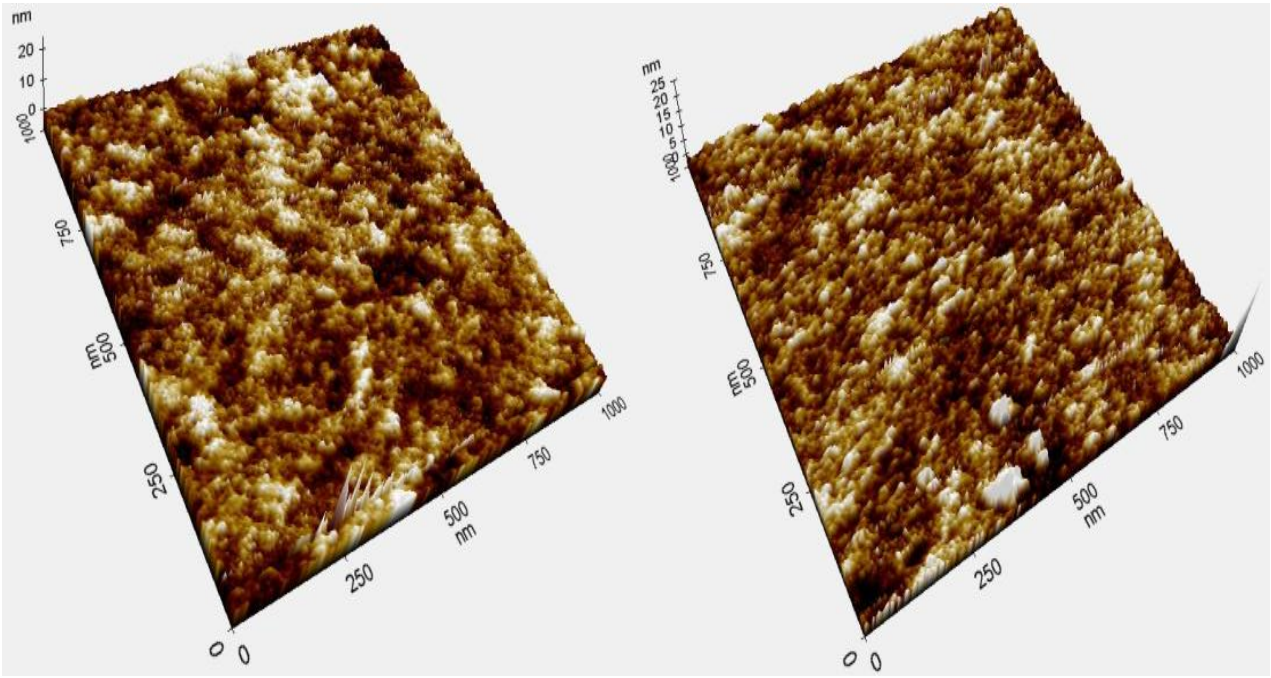

(a) *(b)*

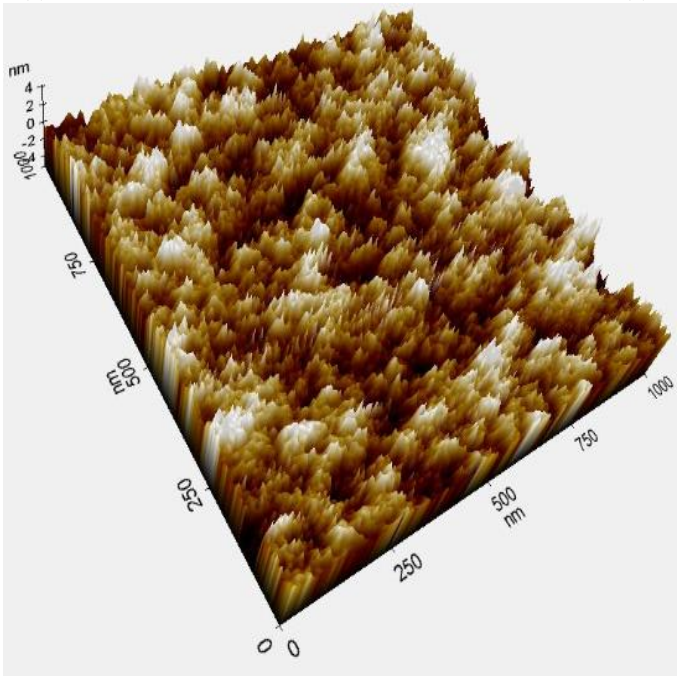

(c)

Fig. 6. The AFM images of a silicon nitride (a) G, (b) H & (c) K (colour online)

The three-dimensional (3D) surface topology image of scanning surfaces is 1x1 μm^2 and obtained results in a height of 25 nm (K), 4.2 nm (G), and 24.2 nm (H), with a corresponding surface area ratio of 2.8, 2.2, and 2.3% [23–24]. At processing temperatures of 800 °C, we have demonstrated the critical thickness of the thin film coatings achieved up to 4 nm ('G' sample). The high surface thicknesses were confirmed at the ends of the side walls ('K' and 'H') as compared to the middle ('G' sample). The samples showed up-and-down surfaces like hills (crests) and valleys (troughs) yielded the large height variation with an average surface roughness of 0.851 nm (K), 0.8 nm (G), and 0.779nm (H) [25]. Naturally, nitride film has a rough surface due to droplets and different heights. Overall, this surface exhibits a relatively high smooth profile as compared to others. However, the smoothness or roughness depends upon the various factors such as residual stress, layer thickness, crystalline size, coalescence, etc. [26–27]. The fabricated Si_3N_4 thin film could be useful in various optoelectronic applications, such as anti-reflection coating in thin film solar cells, as reported by various researchers. These successful preparations of Si_3N_4 thin films on silicon with low reflectance are useful to enhance the absorption within the absorber region. These properties could be

chanced with effect of structural, functional groups of the Si_3N_4 thin films. In prior, we simulated various thin film solar cell performance using the RSoft synopsis tool and reported **[**28–30**].** Particularly, the collection of the photons enhanced up to 22% (cell efficiency) with the addition of Si_3N_4 ARC [31-32]. Also, the effects of current density (Jsc), open circuit voltage (Voc), and cell efficiency are significantly enhanced along with low-cost fabrication.

4. Conclusions

In summary, we fabricated a high-quality crystalline silicon nitride (Si_3N_4) thin film using the chemical vapor deposition (CVD) technique at 800°C. The thin film was deposited on p-type silicon substrates. In the CVD furnace, four different thin film sampleswere fabricated and investigated for their structural, optical, topographical, and functional groups. The UV-visible spectrum showed better anti-reflection coating properties and enhanced up to 15%. The XRD diffraction pattern revealed the crystalline and structural property of $Si_3N_4$with sharp peak which was confirmed α-Si_3N_4 phases. FTIR transmittance spectra were confirmed the significant peak shoulder of 970–1194 cm^{-1}due to the presence of Si_3N_4 molecules. Further, the AFM topography of the samples evidenced the homogenous and well-defined thin film growth on silicon wafer. In the future, these ARC properties would be highly improved with the optimization process, which will be useful in thin film solar cells.

References

[1] Z. Huang, J. Duan, M. Li, Y. Ma, H. Jiang, Coatings **14**(7), 881 (2024).

[2] V. S. Sulyaeva, A. N. Kolodin, M. N. Khomyakov, A. K. Kozhevnikov, M. L. Kosinova, Materials **16**(4), 1467 (2023).

[3] M. Chirumamilla, T. Krekeler, D. Wang, P. K. Kristensen, M. Ritter, V. N. Popok, K. Pedersen, Appl. Nano. **4**(4), 280 (2023).

[4] A. E. Kaloyeros, B. Arkles, ECS J. Solid State Sci. Technol. **13**(4), 043001 (2024).

[5] T. Draher, T.T. Polakovic, J. Li, U. Welp, J.S. Jiang, J. Pearson, W. Armstrong, M. Zein-Eddine, C. Chang, W-K. Kwok, Z. Xiao, V. Novasad, Sci. Rep. **13**, 6315 (2023).

[6] M. M. Islam, A. G. Ranga, V. Borra, D. G. Georgiev, Appl. Phys. A **130**, 376 (2024).

[7] K. W. A. Chee, Z. Tang, H. Lu, F. Huang, Energy Reports **4**, 266 (2018).

[8] N. Ahmed, C. B. Singh, S. Bhattacharya, S. Dhara, P. Balaji Bhargav, Conference Papers in Energy, 1 (2013).

[9] C. C. Lee, S. L. Ku, Applied Optics **49**(3), 437 (2020).

[10] B. Swatowska, T. Stapinski, K. Drabczyk, P. Panek, Optica Applicata **XLI**(2), 487 (2011).

[11] G. Hashmi, M. J. Rashid, Z. H. Mahmood, M. Hoq, Journal of Theoretical and Applied Physics **12**, 327 (2018).

[12] K. C. Sahoo, Y. Li, E. Y. Chang, Men-Ku Lin, Jin-Hua Huang, 2009 International Conference on Simulation of Semiconductor Processes and Devices, 123 (2009).

[13] K. Jhansirani, R. S. Dubey, M. A. More, S. Singh, Results in Physics **6**, 1059 (2016).

[14] R. S. Dubey, K. Jhansirani, S. Singh, Results in Physics **7**, 77 (2017).

[15] S. A. A. Oloomi, A. Saboonchi, A. Sedaghat, International Journal of the Physical Sciences **5**(5), 465 (2010).

[16] T. V. Amotchkina, M. K. Trubetskov, A. V. Tikhonravov, V. Janicki, J. Sancho-Parramon, O. Razskazovskaya, V. Pervak, Opt. Express, 16129 (2012).

[17] S. Duttagupta, F. Ma, B. Hoex, T. Mueller, A. G. Alberle, Energy Procedia **15**, 78 (2012).

[18] E. B. Acousta-Enriquez, M. C. Acosta-Enriquez, R. Castillo-Ortega, M. A. E. Zayas, M. I. Pech-Canul, Dig. J. Nanomater. and Biostruct. **11**(2), 601 (2016).

[19] J. Z. Jiang, K. Sahl, R. W. Berg, D. J. Frost, T. J. Zhou, P. X. Shi, Europhysics Letters **51**(1), 62 (2000).

[20] R. S. Dubey, S. Sigamani, Rasayan Journal of Chemistry **15**(4), 2304 (2022).

[21] J. Z. Jiang, F. Kragh, D. J. Frost, K. Stahl, H. Lindelov, J. Phys.: Condens. Matter. **13**, L515(2001).

[22] J. Marchi, C. Chaves Guedes e Silva, B. B. Silva, Materials Research **12**(2), 145 (2009).

[23] G. Scardera, T. Puzzer, G. Conibeer, M. A. Green, J. Appl. Phys. **104**, 104310-1 (2008).

[24] Sumeyra Savas, Z. Altintas, Materials **12**(2189), 1 (2019).

[25] V. Sunkara, Dong-Kyu Park, Yoon-Kyoung Cho, RSC Advances **2**, 9066 (2012).

[26] K. Abbas, R. Ahmad, I. A. Khan, U. Ikhlaq, S. Saleem, R. Ahson, International Conference on Aerospace Science and Engineering (ICASE). IEEE: Islamabad, Pakistan, 1 (2013).

[27] U. Ikhlaq, R. Ahmad, S. Saleem, M. S. Shah, Umm-i-Kalsoom, N. Khan, N. Khalid, Eur. Phys. J. Appl. Phys. **59**, 20801 (2012).

[28] S. Saravanan, R. S. Dubey, Opt. Commun. **377**, 65 (2016).

[29] S. Saravanan, R. S. Dubey, Materials Today: Proceedings **50**(1), 85 (2022).

[30] S. Saravanan, R. S. Dubey, S. Kalainathan, J. Optoelectron. Adv. M. **19**(3-4), 173 (2017).

[31] S. Saravanan, R. S. Dubey, Nanosyst: Phys. Chem. Math. **8**(4), 503 (2017).

[32] R. S. Dubey, S. Saravanan, Nanosyst: Phys. Chem. Math. **13**(2), 220 (2022).

*Corresponding author: shasa86@gmail.com